Crystallization and structure analysis of *Thermus flavus* 5S rRNA helix B

Marco Vallazza,[a] Sankaran Banumathi,[b] Markus Perbandt,[b] Karen Moore,[c] Larry DeLucas,[c] Christian Betzel[b] and Volker A. Erdmann[a]*

[a]*Freie Universität Berlin, FB Biologie, Chemie, Pharmazie, Institut für Chemie, Thielallee 63, 14195 Berlin, Germany,* [b]*Institut für Medizinische Biochemie und Molekularbiologie, Arbeitsgruppe für Makromolekulare Strukturanalyse, c/o DESY, Notkestraße 85, 22603 Hamburg, Germany, and* [c]*Center for Macromolecular Crystallography, University of Alabama at Birmingham, CBSE 235, 1025 18th Street South, Birmingham, Alabama, 35294-4400, USA.*
E-mail: erdmann@chemie.fu-berlin.de

The crystallization conditions of the synthetic RNA duplex r(GCGGCGU)•r(GCGCCGC), part of the *Thermus flavus* 5S rRNA domain B, were investigated in detail. The crystallization analysis revealed a relativ narrow crystallization zone. Single sequence variations did not enhance the crystal quality, however the crystallization under microgravity provided crystals of higher quality. They belong to the space group $P3_121$ with unit cell dimensions of a = b = 35.0 Å and c = 141.2 Å. Diffraction data up to 2.6 Å were collected and the structure subsequently analyzed and refined to an R-value of 22.4 %. The conformation of the two molecules in the asymmetric unit is stabilized by intermolecular hydrogen bonds. The two molecules A and B are perpendicular to each other and interacting head to tail with symmetry related molecules. They form pseudo-continuous infinite helices in the crystal lattice.

Keywords: **5S rRNA domain, crystallization, microgravity**

1. Introduction

We have focused on contributing to the discovery of novel structural features (Moore, 1999) by determining small RNA structures derived from the ribosomal 5S RNA. In the early 70-ies the interest in this molecule initially arose from observation of a reduced peptidyl transferase activity if ribosomes lack 5S rRNA (Nomura & Erdmann, 1970). However, it took three decades to understand that 5S rRNA is probably assisting in the assembly of the large ribosomal subunit (Khaitovich & Mankin, 1999; Barciszewska *et al.*, 2000). Although the milestone of ribosome structure led to detailed insights into the RNA-protein interaction (Ban *et al.*, 2000), the exact function of the 5S rRNA remained obscure. Further approaches including the crystallization of different domains and their structure at atomic level could reveal new functional properties.

Besides NMR spectroscopy the X-ray structure analysis represents the method of choice for RNA structures. The most challenging step is the growth of large, well-ordered crystals which diffract X-rays to high resolutions. Therefore, several methods have been proposed to stabilize RNA molecules including a tetraloop / tetraloop receptor module for crystallization purposes (Ferré-D'Amaré *et al.*, 1998) or the RNA-protein-complex crystallization (Conn *et al.*, 1999). Another general approach involves the variation of crystallization conditions. Several sparse matrix screens tailored for RNA are commercially available containing either empirically proven solutions or a set of new combinations of favorite components (precipitant, ions, buffer, polyamine). Nevertheless, the RNA crystallization remains a difficult trial and error process. Once crystals are obtained, a subsequent optimization can also be performed in microgravity which largely reduces the convection and the sedimentation of crystal nuclei in the drop with the consequence that well-ordered crystal lattices and higher packing densities can be formed.

Short RNA fragments up to 25 nucleotides can be easily crystallized using commercial screens, and they often diffract to high resolution (Cruse *et al.*, 1994; Anderson *et al.*, 1996; Biswas *et al.*, 1997). X-ray studies were performed by our group on the domains A, C and E of *Thermus flavus* 5S rRNA, especially analyzing the influence and function of solvent water (Barciszewski *et al.*, 1999). In detail, the importance of highly ordered internal water molecules in the fragment A for the stabilization of the RNA helix was demonstrated (Betzel *et al.*, 1994). Furthermore, G:U wobble base pairs in tandem formation are stabilized by highly conserved structural waters (Perbandt *et al.*, 1999), and a G:C base pair appeared in a wobble-like conformation enabled by the protonation of cytidine (Perbandt *et al.*, 2001).

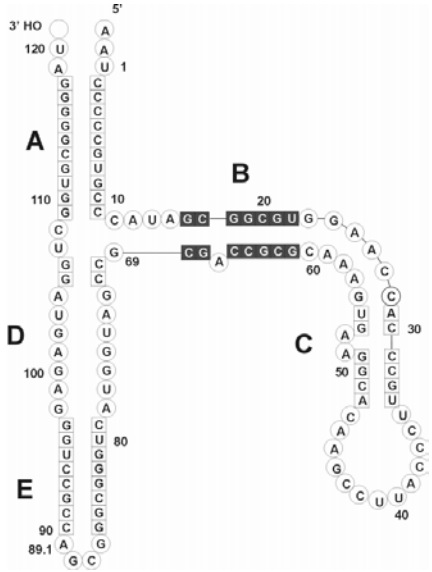

Figure 1

Secondary structure model of *Thermus flavus* 5S rRNA. The 7 bp helix of the domain B is white-typed.

The present structure involves a 7 bp double helix of the *Th. flavus* 5S rRNA domain B with the exclusion of the bulge nucleotide occurring in the native sequence (Fig. 1). The duplex contains a G:U wobble base pair followed by six G:C Watson-Crick base pairs. The crystallization in particular and the structure analysis are presented.

2. Material and methods

2.1. RNA synthesis, crystallization and data collection

Standard phosphoramidite chemistry was used for the synthesis of oligoribonucleotides. In order to hybridize aquimolar amounts of RNA strands, the oligoribonucleotide concentrations were exactly calculated by the Lambert-Beer equation. The specific extinctional coefficients $\varepsilon_{\text{nt 16-22}} = 56685\ \text{l*mol}^{-1}\text{*cm}^{-1}$ and $\varepsilon_{\text{nt 61-68}(\Delta 66)} = 52579\ \text{l*mol}^{-1}\text{*cm}^{-1}$ were determined by alkaline hydrolysis as previously described (Vallazza *et al.*, 2001). The RNA strands were mixed to a

final concentration of 0.5 mM in bidestilled water, subsequently incubated at 90°C for 1 min and slowly cooled to room temperature over night.

Crystallization trials were performed by using the hanging drop vapor diffusion technique at 4°C, 18°C and 32°C. The drop size of 2 µl was obtained by combining 1µl RNA with 1µl crystallization solution. For the initial screening several commercial screens (Hampton Research, Jena Bioscience) and the sparse matrix screens described in the literature (Doudna *et al.*, 1993; Scott *et al.*, 1995; Berger *et al.*, 1996) were applied. Within three days well-shaped crystals grew at 18°C in conditions based on 2-methyl-2,4-pentanediol (MPD). This fact enabled the application of a self-developed screening protocol on MPD precipitation which was previously published by our group (Vallazza *et al.*, 2001). Finally, 40 mM sodium cacodylate (pH 7.2), 10 % (v/v) MPD, 100 mM spermine tertrahydrochloride and 80 mM NaCl proved to be the best suited condition for the crystal growth of the helix B1 r(GCGGCGU)•r(GCGCCGC). The hanging drop was equilibrated against 30 % (v/v) MPD.

Finally, three crystallization experiments were performed at 22°C under microgravity conditions using **H**igh **D**ensity **P**rotein **C**rystal **G**rowth (HDPCG) hardware and the **m**odified **C**ommercial **I**ncubator/**R**efrigerator **m**odule (CRIM-M) supplied by NASA. The HDPCG reactor consisted of a cell body and a cell barrel which carried the insert for the macromolecule. The cell barrel could be rotated 180° from the filling position to the activated position giving contact between the drop and the reservoir. A maximum volume of 550 µl reservoir solution was taken up by a porous polymer. The crystallization on the International Space Station (ISS-6A) lasted from April 21st (STS-100) to August 19th 2001 (STS-105). To adjust the crystal growth to the long period in space the vapor diffusion kinetics were slowed down by means of a lower precipitant concentration (20 % MPD) and an enlarged drop size of 16 µl (8 µl RNA plus 8 µl buffer). The crystal morphology is hexagonal platelets with dimensions of 0.1 x 0.1 x 0.02 mm (Fig. 2).

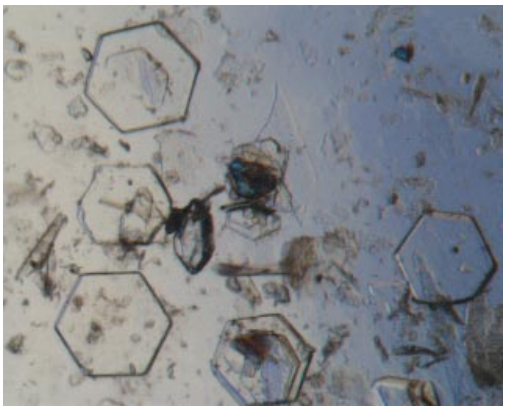

Figure 2

Space crystals of the 7 bp helix B1. The crystal size is 0.1 x 0.1 x 0.02 mm.

Diffraction data for the space crystals were collected at 100 K with synchrotron radiation (λ = 1.0 Å) at DESY/X13 (Hamburg), whereas all other crystals were analyzed at ELETTRA/5.2R (Trieste). The 30 % MPD present in the crystallization solution are a sufficient cryoprotectant. The data processing was done by using the program DENZO (Otwinowski & Minor, 1997). The space group was assigned as $P3_221$ or the enantiomeric one $P3_121$. The packing parameter V_M for two molecules was calculated to be 3.0 Å^3/Da (Mathews, 1968).

2.2. Structure solution and refinement

The structure was solved by molecular replacement using the program package AMoRe (Navaza, 1994). The X-ray structure of 5S rRNA helix E (Perbandt *et al.*, 2001) was used as a search model after its sequence was adjusted to helix B manually. For the space group $P3_121$ a clear solution was found. The correlation factor was 62.3 (R-factor 40.7 %) in the resolution range from 8.0 to 3.5 Å for two duplexes in the asymmetric unit. The enantiomeric space group $P3_221$ gave no solution for the molecular replacement. Rigid body refinement and consequent positional least-squares refinement using REFMAC (Murshudov *et al.*, 1997) in the resolution range from 8.0 to 3.0 Å dropped the R and R_{free} to 28.3 and 33.1 %. The initial overall B-factor of the molecules was 66 Å^2 calculated by REFMAC. Further refinement applying X-PLOR (Brünger, 1992) dropped the isotropic B-refinement to 37.8 Å^2. The resolution range used for the refinement was extended to 2.6 Å. Water molecules were manually identified in the Fo-Fc difference electron density map at the 3σ level. Some of them were removed if they failed to reappear at the 1σ level in the 2Fo-Fc map. The model building and insertion of 24 water molecules reduced the R and R_{free} to 22.3 and 27.4 %. Finally, omit maps were calculated for confirming the density for the base pairs. A summary of the data collection parameters and refinement is listed in Table 1.

Table 1 Refinement statistics and quality of the model.

Parameter	Data
Unit cell dimensions (Å)	
a = b =	35.0
c =	141.2
Space group	$P3_121$
V_m (Å^3/Da)	3.0
Resolution range (Å)	25.0 - 2.6
Total number of reflections	2507
Number of reflections$_{\text{used for refinement}}$	2362
R-value (%)	22.3
R_{free} (%)	27.4
Model	
Nucleic acid atoms	590
Water molecules	24
Average B value (Å²)	
of all atoms	38.7
of molecule A	36.2
of molecule B	39.4
of water atoms	62.0
of backbone atoms	42.1
of side chain atoms	33.4
RMS deviation from ideal geometry	
Bond length (Å)	0.02
Bond angles (°)	5.3
Dihedral angles (°)	11.9

3. Results and discussion

3.1. Crystallization

Several helical structures which include a bulged adenosine or an overhanging nucleotide were tried to be crystallized. They were termed B1: r(GCGGCGU)•r(GCGCCGC), B2: r(GCGGCGU)•r(GCGCCAGC), B3: r(CCGCGGCG)•r(CGCCAGCGG) and B4: r(UGGCGGCG)d^{Br}U•r(CGCCAGCCA)d^{Br}U. However, among these different fragments of the domain B only the 7 bp helix B1 lacking the bulge adenosine could be crystallized (Fig. 2). Neither the original sequence (B2) nor the structurally stabilized variants containing multiple G:C base pairs on both sides of the bulge (B3) or an overhanging 5'-desoxyBromo-uridine at the 3'-end (B4) resulted

in any crystals applying several commercial and self-developed screens. In general, the bulge nucleotide may intercalate or turn outside the helix. Both conformational changes cause a helix kinking and the weakening of base pairs in the direct neighborhood of the bulge (Lilley, 1995). A couple of strong G:C bp on both sides of the bulged adenosine did not compensate the flexibility of the domain B. Similarly, the stabilization by an intermolecular helix stacking at overhanging bases did not work (Cruse *et al.*, 1994; Anderson *et al.*, 1996).

The presence of a polyamine like spermine tetrahydrochloride ($SpCl_4$) or cobalt hexaminchloride proved to be essential for the appearance of B1 crystals although $SpCl_4$ was not visible in the final crystal structure. Besides, the ion composition exerted a strong influence on the crystallization. Whereas $MgCl_2$ strictly prevented crystal growth, other divalent ions (Ba^{2+}, Ca^{2+}, Co^{2+}) were favorable as companion of sodium. In contrast, monovalent ions (Na^{+}, K^{+}, Li^{+}) could cause crystallization without divalent support. The derivation of general RNA crystallization rules seems to be more complex (Vallazza *et al.*, 2001).

The size and shape of the ground controls compared to the space crystals were quite similar. However, the space crystals diffracted to a maximum resolution of 2.6 Å in contrast to 4.0 Å of the ground controls or 2.9 Å of the crystals grown on Earth before ISS-6A. This result supports the NASA statistics stating that about 37 % of space crystals achieved a better resolution than it was ever obtained on Earth.

3.2. Overall structure description

The helical parameters were calculated using the program NEWHEL. The two molecules (Fig. 3) were superimposed and the r.m.s. deviation was found to be 1.0 Å which indicates that two molecules adopt almost identical conformations. This fact was also confirmed by the close similarity of the helical parameters in both molecules (Table 2).

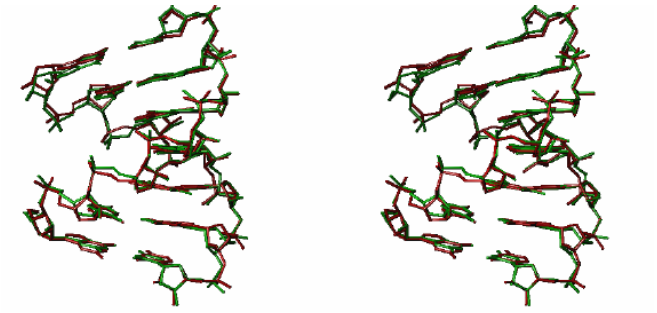

Figure 3

The stereo view of the superposition of the molecules A and B.

The high standard and the angular deviations are the consequence of the high thermal parameter which also reflects the quality of the crystal. There is no irregular hydrogen bonding between the base pairs and hence there is no loss of Watson-Crick base pair formation. The p-p distances and the helical parameters conforms with the A' RNA.

The packing diagram (Fig. 4) shows the final model emphasizing that there is little irregularity in the helix formation. The sugar puckering is C3'–endo, C3'-endo–4'-exo 2'-exo–3'-endo unlike the puckering observed in domain E (Table 2). The torsion angles α and γ are g^{-} and g^{+}, respectively.

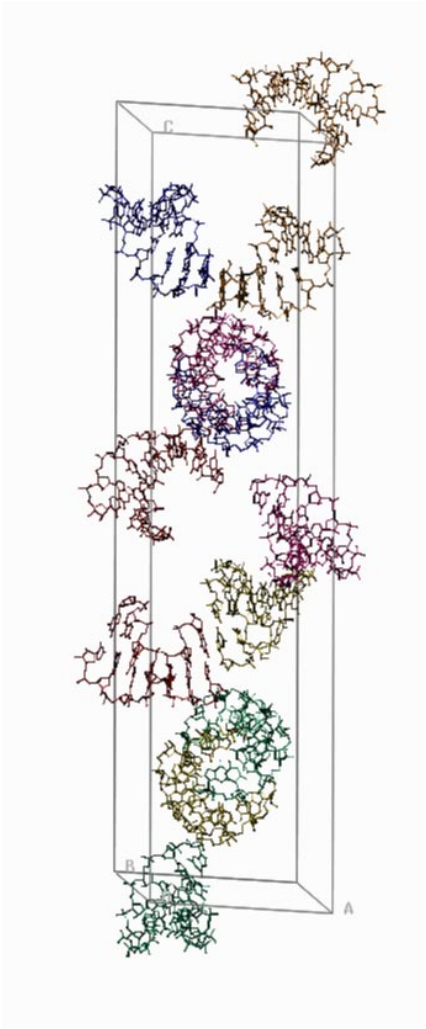

Figure 4

The packing of the molecules in the unit cell along the b axis.

Table 2

Average values of helical parameters

	Twist (°)	Rise (Å)	X-Dsp (Å)
Molecule A	30.3 (41)	2.7 (3)	-4.5 (12)
Molecule B	30.9 (13)	2.7 (5)	-4.2 (14)
A'-RNA	30.0	3.0	4.4
Domain E of 5S rRNA			
Molecule A	30.6 (11)	3.4 (5)	5.8 (19)
Molecule B	30.9 (10)	3.2 (4)	5.5 (27)
Domain A of 5S rRNA	33.3 (47)	2.4 (5)	4.5 (5)
tRNA (mono)	33.5	2.41	4.4

3.3. Structural features

The two duplexes pack in a familiar head to tail fashion with their symmetry related to double helices. They are forming independent pseudo-continuous infinite RNA helices which are mutually perpendicular to each other. In general, the molecular arrangement in the head to tail fashion results in a continuous and regular helix compared to the molecules packed in the head to head fashion (Biswas *et al.*, 1997). There are some exceptions concerning this observation when one end of the helix is closed by a loop exhibiting head to tail packing arrangement with indefinite layer of antiparallel helices (Perbandt *et al.*, 1998). The pseudo-continuous helices are

interacting with their neighbouring double helices through N-H---O and O-H---O intermolecular hydrogen bonds. The ribose ring oxygen O4 atom of GUA 61B of one strand acts as a donor and forms N-H---O and O-H---O hydrogen bonds with the N1 and N3 atoms of the CYT 67B (molecule B) of the symmetry related (y, x, -z) molecule with the distances 3.20, 3.07 and 3.23 Å, respectively. In the same way the interaction occurs in the other strand between GUA 16A and URA 22A (molecule A).

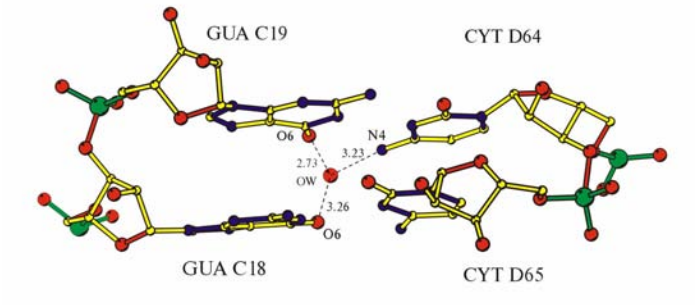

Figure 5

The packing of the molecules in the unit cell along the b axis.

The base pairs GUA 19C, GUA 18C and CYT 64D in molecule B are stabilized by one water molecule named 4OW (Fig. 5; Table 3).

Table 3

Water molecule interaction with the molecules A and B

Water molecule	Source atoms	Distance angle
4 OW	GUA 18C O6	3.26
	GUA 19C O6	2.73
	CYT 64D N4	3.23
3 OW	URI 22C O2P	3.03
12 OW	CYT 20C O2'	3.37
13 OW	GUA 66B O6	2.55
17 OW	URI 22A O3'	3.02
18 OW	CYT 67B O3'	3.17

4. Conclusions

Several similar RNA helices including irregularities and overhangs were tested for their crystallization behavoir. Obviously, marginal sequence variations could already exert a significant influence on the crystal growth (Scott *et al.*, 1995) and might diminish the efforts in screening a suited crystallization condition (Higgins & Linton, 2001). Once crystals were obtained, systematic changes of the buffer composition or the reduction of the growth rate were some helpful tools for their further optimization. The increased resolution of the space crystal B1 compared to the ground control can be addressed to microgravity (Lorenz *et al.*, 2000) as the beamlines ELETTRA/5.2R and DESY/X13 provide almost the same intensity. The structure presented here shows again that the principles of RNA folding and conformation are important features determining RNA structure and function. Therefore, it is of great interest to indicate and recognize structural RNA motifs that are responsible for the mediation of intermolecular contacts and are essential for RNA folding and function.

We thank the staff of the X-ray beamlines at DESY/Hamburg as well as at ELETTRA/Trieste for the opportunity of crystal analysis. The work was supported by the Deutsche Luft- und Raumfahrt-agentur (DLR) and the Fonds der Chemischen Industrie e.V..

References

Anderson, A. C., Earp, B. E. & Frederick, C. A. (1996). *J. Mol. Biol.* **259**, 696-703.

Ban, N., Nissen, P., Hansen, J., Moore, P. B. & Steitz, T. A. (2000). *Science* ,**289**, 905-920.

Barciszewska, M. Z., Szymanski, M., Erdmann, V. A. & Barciszewski, J. (2000). *Biomacromolecules*, **1**, 297-302.

Barciszewski, J., Jurczak, J., Porowski, S., Specht, T. & Erdmann, V. A. (1999). *Eur. J. Biochem.* **260**, 293-307.

Berger, I., Kang, C., Sinha, N., Wolters, M. & Rich, A. (1996). *Acta Cryst.* D**52**, 465-468.

Betzel, C., Lorenz, S., Fürste, J. P., Bald, R., Zhang, M., Schneider, T. R., Wilson, K. S. & Erdmann, V. A. (1994). *FEBS Lett.* **351**, 159-164.

Biswas, R., Wahl, M. C., Ban, C. & Sundaralingam, M. J. (1997). *J. Mol. Biol.* **267**, 11449-11456.

Brünger, A. T. (1992). *X-PLOR. Version 3.1. A system for crystallography and NMR.* Yale University Press, New Haven.

Conn, G. L., Draper, D. E., Lattman, E. E. & Gittis, A. G. (1999). *Science* ,**284**, 1171-1174.

Cruse, W. B. T., Saludjian, P., Biala, E., Strazewski, P., Prange´, T. & Kennard, O. (1994). *Proc. Natl Acad. Sci. USA*, **91**, 4160-4164.

Doudna, J. A., Grosshans, C., Gooding, A. & Kundrot, C. E. (1993). *Proc. Natl Acad. Sci. USA*, **90**, 7829-7833.

Ferré-D'Amaré, A. R., Zhou, K. & Doudna, J. A. (1998). *J. Mol. Biol.* **279**, 621-631.

Higgins, C. F. & Linton, K. J. (2001). *Science*, **293**, 1782-1784.

Khaitovich, P. & Mankin, A. S. (1999). *J. Mol. Biol.* **291**, 1025-1034.

Lilley, D. M. J. (1995). *Proc. Natl Acad. Sci. USA*, **92**, 7140-7142.

Lorenz, S., Perbandt, M., Lippmann, C., Moore, K., DeLucas, L., Betzel, C. & Erdmann, V. A. (2000). *Acta Cryst.* D**56**, 498-500.

Mathews, B.W. (1968). *J. Mol. Biol.* **33**, 491-497.

Moore, P. B. (1999). *Annu. Rev. Biochem.* **68**, 287-300.

Murshudov, G. N., Vagin, A. A. and Dodson, E. J. (1997). *Acta Cryst.* D**53**, 240-255.

Navaza, J. (1994). *Acta Cryst.* D**50**, 157-163.

Nomura, M. & Erdmann, V. A. (1970). *Nature (London,)* **228**, 744-748.

Otwinowski, Z. & Minor, W. (1997). *Methods Enzymol.* **276**, 307-326.

Perbandt, M., Nolte, A., Lorenz, S., Bald, R., Betzel, C. & Erdmann, V. A. (1998). *FEBS Lett.* **429**, 211-215.

Perbandt, M., Lorenz, S., Vallazza, M., Erdmann, V. A. & Betzel, C. (1999). In: J. Barciszewski and B.F.C. Clark (eds.) *RNA Biochemistry and Biotechnology*, pp. 63-71. Kluwer Academic Publishers.

Perbandt, M., Vallazza, M., Lippmann, C., Betzel, C. & Erdmann, V. A. (2001). *Acta Cryst.* D**57**, 219-224.

Scott, W. G., Finch, J. T., Grenfell, R., Fogg, J., Smith, T., Gait, J. & Klug, A. (1995). *J. Mol. Biol.* **250**, 327-332.

Vallazza, M., Senge, A., Lippmann, C., Perbandt, M., Betzel, C., Bald, R. & Erdmann, V. A. (2001). *J. Cryst. Growth*, **232**, 340-352.